

## Claremont Colleges Scholarship @ Claremont

---

All HMC Faculty Publications and Research

HMC Faculty Scholarship

---

1-1-1994

# Optical Properties of Human Uterus at 630 nm

Steen J. Madsen

*University of California - Irvine*

Bruce J. Tromberg

*University of California - Irvine*

Yona Tadir

*University of California - Irvine*

Pius Wyss

*University Hospital of Zurich*

Lars O. Svaasand

*University of Trondheim*

*See next page for additional authors*

---

### Recommended Citation

Madsen, SJ, Tromberg, BJ, Tadir, Y, Wyss, P, Svaasand, LO, Haskell, RC. Optical properties of human uterus at 630 nm. In: Alfano RR, editor. OSA proceedings on advances in optical imaging and photon migration: proceedings of the topical meeting, March 21-23, 1994, Orlando, Florida. Vol. 21. Washington, D.C.: Optical Society of America, 1994. p. 262-264.

This Conference Proceeding is brought to you for free and open access by the HMC Faculty Scholarship at Scholarship @ Claremont. It has been accepted for inclusion in All HMC Faculty Publications and Research by an authorized administrator of Scholarship @ Claremont. For more information, please contact [scholarship@cuc.claremont.edu](mailto:scholarship@cuc.claremont.edu).

---

**Authors**

Steen J. Madsen, Bruce J. Tromberg, Yona Tadir, Pius Wyss, Lars O. Svaasand, and Richard C. Haskell

# Optical Properties of Human Uterus at 630 nm

Steen J. Madsen, Bruce J. Tromberg, and Yona Tadir

Beckman Laser Institute, University of California-Irvine, Irvine, California 92715

Pius Wyss

University Hospital of Zurich, 8093 Zurich, Switzerland

Lars O. Svaasand

University of Trondheim, 7000 Trondheim, Norway

Richard C. Haskell

Harvey Mudd College, Claremont, California 91711

## Abstract

The optical properties of normal and fibrotic human uteri were determined using frequency-domain and steady-state techniques.

## Introduction

The study of light propagation in tissue has become important due to the increasing use of lasers and other light sources in many medical and biological applications. Absorption and scattering of light determine its spatial distribution within the irradiated tissue and the subsequent biological effects in therapeutic uses such as laser surgery [1] and photodynamic therapy [2]. In diagnostic applications, the light that is remitted (i.e., diffusely reflected from or transmitted through the tissue, can be measured to probe the metabolic) physiologic, or perhaps the structural status of the tissue.

From a clinical point of view, the optical properties (the absorption ( $\mu_a$ ) and transport scattering ( $\mu'_s$ ) coefficient in this case) of the irradiated tissue should be determined noninvasively. This is possible using time- or frequency-domain techniques in which the perturbation of short light pulses (time-domain) or sinusoidally amplitude-modulated light waves (frequency-domain) travelling through multiple scattering media, such as biological tissue, are compared to the predictions of appropriate models of light propagation.

In this study, the optical properties of both normal and fibrotic (nonneoplastic) human uteri were investigated using frequency-domain photon migration (FDPM) and steady-state techniques. In all cases, the propagation of light was modeled as a diffusive process.

## Theory

### (i) Frequency-domain photon migration

In frequency-domain measurements, the phase lag and demodulation amplitude with respect to a source response are recorded. These measurable quantities are functions of the angular modulation frequency ( $\omega$ ), the source-detector separation ( $r$ ) and the optical properties of the medium. In an infinite tissue-like medium, at sufficiently low modulation frequency ( $\omega \ll m_a c$ ), the phase velocity of the photon

density waves ( $V_p$ ) reaches a dispersionless lower limit independent of modulation frequency<sup>3</sup>:

$$V_p = 2\mu_a c \delta \quad (1)$$

where  $c$  is the speed of light in tissue ( $n = 1.40$ ) and  $\delta$  is the dc penetration depth,

$$\delta = [3\mu_a(\mu_a + \mu'_s)]^{-1/2} \quad (2)$$

The phase velocity and phase slope (slope of phase vs. frequency plot) are related by<sup>3</sup>

$$\alpha = \frac{r}{V_p} \quad (3)$$

where  $\alpha$  is the phase slope. Thus measurement of the phase slope as a function of fiber separation yields  $V_p$ .

### (ii) Steady-state

If the source and detector fibers are separated by a sufficient distance such that diffusion theory is valid, the fluence rate ( $f$ ) will decay exponentially with source-detector separation:

$$\phi(r) = \frac{\phi_0}{r} \exp\left(-\frac{r}{\delta}\right) \quad (4)$$

where  $f_0$  is the fluence rate at some initial separation. Thus a

plot of  $\ln\left(\frac{\phi_0}{r\phi(r)}\right)$  vs.  $r$  yields a straight line with slope  $1/\delta$ .

## Materials and Methods

### (i) Instrumentation

The photon migration instrument used in these experiments (Fig. 1) has been described extensively elsewhere [3]. Briefly, a Pockels cell (PC) driven by a harmonic comb generator (HCG1) is used to produce high harmonic content pulses from

a continuous wave argon ion pumped dye laser ( $\lambda = 630 \text{ nm}$ ). The pulses are launched into the sample through a flat-cut 600  $\mu\text{m}$ -dia. fused silica fiber (F1). A small portion of the light is diverted to a reference photomultiplier tube (PMT<sub>r</sub>) which allows phase and modulation locking of the instrument.

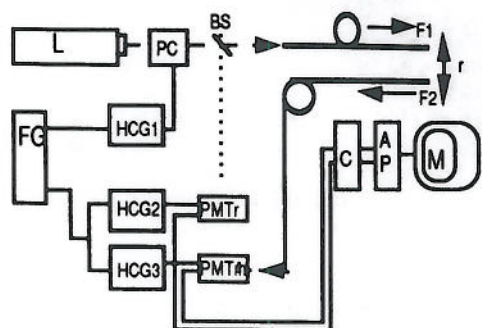


Figure 1. Frequency-domain instrument. BS = beam splitter, M = display monitor, L = laser, FG = frequency generator.

Scattered light is collected by a second fiber (F2) identical to F1 and transmitted to the measurement photomultiplier tube (PMT<sub>m</sub>). The gain of the detectors is modulated by HCG2 and HCG3 at a small frequency offset (3 Hz). The sample's phase and amplitude response at each harmonic is contained within these cross-correlation frequencies which are sampled and digitized by a dual-channel analog-to-digital converter (C). The digital data is converted to a frequency spectrum by an array processor (AP). The total time required to obtain phase and modulation data from 50 frequencies up to 250 MHz is approximately 30 seconds.

(ii) Measurements

Intact uteri were obtained immediately following hysterectomy and placed on ice. Ex vivo measurements were performed on six cold, fresh specimens (1 post- and 5 pre-menopausal). Samples were returned to the pathologist for tissue analysis upon completion of the measurements (typically 3-4 hours). Both frequency-domain and steady-state measurements were made in transmittance mode, i.e., with the source and detector fibers inserted into the tissue and facing each other. The source fiber was inserted in the myometrial layer approximately 10 mm into the uterus while the detector fiber was inserted from the opposite side until it was approximately 5 mm from the source. Fibroid data were acquired from a large (3.5 cm dia.) round structurally distinct fibrotic tumor.

In the case of the frequency domain measurements, phase vs. frequency spectra were obtained as a function of source-detector separation by backing the detector fiber away from the source using a micropositioner. Measurements were repeated five times at each source-detector separation. The upper cut-off frequency (typically between 90 and 130 MHz) for the determination of the phase slope was based on the best linear fit to the data as judged by the correlation coefficient.

In the steady-state measurements, the light beam was steered around the Pockels cell and launched directly into the source fiber. The detector fiber was moved in increments of either 1 or 2 mm and the dc intensity recorded.

Results and Discussion

Results of the phase slope vs. source-detector fiber separation are illustrated for a representative pre-menopausal sample in Fig. 2. Each data point represents the mean of five measurements and the solid line is a linear fit to the data. As expected, the phase slope increases linearly with fiber separation. The phase velocity was extracted from the slope of this plot.

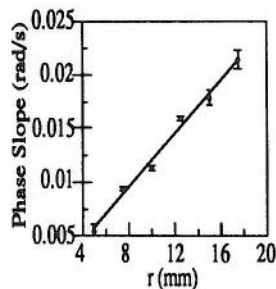


Fig. 2

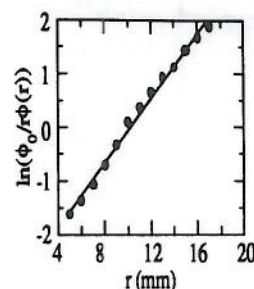


Fig. 3

Figure 2. Phase slope vs. fiber separation.

Figure 3. Steady-state penetration depth measurements.

Results of the steady-state penetration depth measurements are illustrated for the same sample in Fig. 3. The penetration depth was determined from the slope of the best fit line according to Eq. (4). The optical properties of the bulk uterus were then determined by combining the expressions for the phase velocity [Eq. (1)] and penetration depth [Eq. (2)]. The results are summarized in Table 1. There appear to be significant differences in the penetration depth, phase velocity and absorption coefficient between the three different tissue types (post- and pre-menopausal myometrium and fibroid).

Absorption differences between the three tissue types were probably due to differences in water and hemoglobin content. For example, the post-menopausal uterus was much smaller and tougher than the other tissues indicating a reduced water content. The low absorption coefficient of the fibroid indicates a lack of hemoglobin compared to the other tissues. No significant differences in the transport scattering coefficients were observed, although the dense, shrunken post-menopausal uterus had slightly higher  $m'_s$  values than some of the pre-menopausal and fibroid samples. We are currently comparing the size and density of cells in each sample using conventional histological techniques.

Table 1. Optical parameters of the uterus

sample	no. of samples	Penetr. Depth (mm)	Phase vel. (mm/s)	Abs. Coeff. (mm <sup>-1</sup> )	Scatt. Coeff. (mm <sup>-1</sup> )
post-menop.	1	2.59±0.26	(5.72±0.17)* 10 <sup>10</sup>	(5.15±0.54)* 10 <sup>-2</sup>	0.91±0.17
pre-menop.	4	4.79±0.32	(3.96±0.07)* 10 <sup>10</sup>	(1.93±0.13)* 10 <sup>-2</sup>	0.73±0.09

		3.39± 0.28	(4.56± 0.22)* 10 <sup>10</sup>	(3.14± 0.30)* 10 <sup>-2</sup>	0.89± 0.15
		5.11± 0.20	(4.65± 0.49)* 10 <sup>10</sup>	(2.13± 0.24)* 10 <sup>-2</sup>	0.60± 0.08
		4.77± 0.45	(4.02± 0.49)* 10 <sup>10</sup>	(1.97± 0.30)* 10 <sup>-2</sup>	0.73± 0.15
fibroid	1	7.46± 0.43	(2.63± 0.18)* 10 <sup>10</sup>	(8.24± 0.75)* 10 <sup>-3</sup>	0.72± 0.09

Inter sample differences may be due to differences in the stage of the menstrual cycle at which the measurements were made. The uterus is under hormonal control and undergoes significant morphological change (including blood content) during the cycle. Unfortunately, the stage of the menstrual cycle was not known since the surgeon does not record this prior to the hysterectomy.

In principle, it should be possible to obtain the optical properties of biological tissues non-invasively using surface measurements. Such attempts were made in the frequency domain. Expressions derived from diffusion theory relating the phase lag and demodulation to the optical properties were fit to

the experimental data. However, due to the limited frequency range of the instrument (up to 250 MHz), the demodulation was insufficient to yield the optical properties [3]. We are currently developing a 500 MHz diode laser-based system in order to overcome this limitation.

#### Acknowledgements

This work was supported by the Whitaker Foundation (WF16493), Beckman Instruments Inc., The National Institutes of Health (R29GM50958), the Office of Naval Research (N00014-91-0134), and the Department of Energy (DE-FG-3-91-ER61227). The authors are grateful to the following for their assistance: Alexander Karn, Eric Cho, David Pham, Cuong Ly, and Tuan Ho.

#### References

1. S.L. Jaques and S.A. Prael, "Modeling optical and thermal distributions in tissue during laser irradiation," *Lasers Surg. Med.* **6**, 494-503 (1987).
2. B.C. Wilson and M.S. Patterson, "The Physics of Photodynamic Therapy," *Phys. Med. Biol.* **31**, 327-360 (1986).
3. B.J. Tromberg, L.O. Svaasand, T.T. Tsay, and R.C. Haskell, "Properties of photon density waves in multiple scattering media," *Appl. Opt.* **32**, 607-616 (1993).